GEOPHYSICAL RESEARCH LETTERS, VOL. 23, NO. 15, PAGES 1905-1908, JULY 15, 1996

A 2-D model simulation of downward transport of NO_y into the stratosphere: Effects on the 1994 austral spring O_3 and NO_y

Linwood B. Callis,[1] Daniel N. Baker,[2] Murali Natarajan,[3] J. Bernard Blake,[4]
Richard A. Mewaldt,[5] Richard S. Selesnick,[5] and Jay R. Cummings[5]

Abstract. Simulations using SAMPEX and HALOE data suggest that NO_y produced by thermospheric processes and by relativistic electron precipitation in the mesosphere and lower thermosphere have been important to stratospheric NO_y and O_3 during the austral spring in 1994. The relative importance of the two NO_y sources is discussed. The results are supported by an analysis of HALOE NO_x and CH_4 data during October 1994 and are in agreement with ATMOS NO_y observations made in November 1994.

Introduction

It has been suggested that there is a possible coupling between the thermosphere, mesosphere, and stratosphere by means of the downward transport of odd nitrogen (NO_y), at high latitudes, during periods of advective descent [*Solomon et al.*, 1982; *Garcia et al.*, 1984; *Russell et al.*, 1984; *Callis et al.*. 1986, 1991*a,b*]. *Callis et al.* [1996, this issue] have provided evidence of the effects of precipitating electrons on mesospheric and thermospheric NO_y. With 2-D simulations, this paper examines the contributions to stratospheric NO_y made by the downward transport of NO_y, formed by thermospheric processes and by electron precipitation. The simulations use satellite observations of both thermospheric NO from HALOE and NO source profiles derived from electron fluxes observed by the Solar Anomalous Magnetospheric Particle Explorer (SAMPEX).

2-D Model

Simulations in this study used a modified version of the model described in *Callis et al.* [1991 *a,b*] extended to ≈100 km. Diabatic transport fields are derived from heating rates which are calculated using SBUV ozone and an NMC temperature climatology for the stratosphere. MSIS is used for mesospheric temperatures. Non-LTE effects are included in the calculation of the CO2 cooling rates according to *Zhu et al.* [1992]. Heating efficiencies given by *Mlynczak and Solomon* [1993] have been adopted in the evaluation of solar heating and chemical heating due to exothermic reactions. Stratospheric horizontal mixing coefficients are based on *Yang et al.* [1990], and in the mesosphere these are set equal to the upper stratospheric values. Vertical diffusion is negligible in the stratosphere, but values of $\approx 10^6$ (cm^2/sec) are used in the mesosphere.

We include reactions involving species from the O_x, NO_x, HO_x, Cl_x, and Br_x families. The upper boundary condition for O_x is derived from the MSIS reference atmosphere. Averaging factors are used to account for diurnal variations. Heterogeneous chemical effects on sulfate aerosols are included for a background aerosol distribution. The kinetic rates and cross-sections used are taken from *DeMore* [1992]. We include a parameterized ozone hole [*Callis et al.*, 1991*b*] and denitrification. Denitrification occurs with a 30 day time constant from Julian day 153 to 288 and from 14 to 24.5 km. The NO_y to which the parameterization relaxes was taken to be 0.2 ppbv. The three simulations which we use in this analysis are described in Table 1.

Data

The SAMPEX mission is described by *Baker et al.* [1993] and a description of the PET (Proton Electron Telescope) instrument is provided by *Cook et al.* [1993]. It provides electron measurements from 0.40 to 15 MeV with coverage between ±82°and at all longitudes. The satellite pointing strategy and PET angular response is such that the instrument reflects both precipitating and trapped electron populations as well Long-term at-

Table 1. Summary of Simulations

Simulation	Description
1	SS[1],NO_y from N_2O, 1990 trace gases, zero NO_y flux at upper b.c.
2	SS, same as 1 except HALOE NO for upper b.c.
3	TD[1], same as 2 including electron source of NO_y

[1] SS = steady state, TD = time dependent

[1] ASD, NASA-Langley Research Center, Hampton, VA 23681 USA
[2] LASP, University of Colorado, Boulder, CO 80303
[3] SAIC, Hampton, VA 23666
[4] Aerospace Corp., Los Angeles, CA 90009
[5] SRL, Cal. Tech., Pasadena, CA 91125

Paper number 96GL01788
0094-8534/96/96GL-01788$05.00

mospheric energy inputs are derived from PET as follows. Assume a two-part exponential spectrum with e-folding energies, $E_{O,L}$ and $E_{O,H}$ for $0.4 \leq E \leq 1.0$ MeV and $1.0 \leq E \leq 15$ MeV, respectively. Using PET electron fluxes, P1, ELO, and EHI, derive daily averaged values of $E_{O,L}$ and $E_{O,H}$ over the South Atlantic Anomaly (SAA) and over $3.0 \leq L \leq 6.0$ (L is the McIlwain parameter, see *McIlwain* [1961]). With the daily average of the integral electron flux, derive the multiplying constant for the exponential spectra. Calculate the global magnetospheric energy (GME) for the SAA and outer trapping region of the magnetosphere. Declines in GME from one day to the next, are assumed to be energy lost to the atmosphere. The average of all such declines observed in the long-term record is then conservatively assumed to be occurring during those days when there is an increase in GME. Energy input is apportioned between hemispheres according to the areas of the SAA and the region for $3.0 \leq L \leq 6.0$. Energy deposition profiles can be calculated for each day from which the NO_y source profiles for each hemisphere may be determined and used in the time dependent simulations extending from 920720 through 950515.

Some of the results of this approach are illustrated on Figure 1. The thin line on Figure 1 presents the total energy obtained in this way in NO_y equivalents, i. e. the total number of molecules of NO_y that could be formed were all of this energy used in the formation of ion pairs in the atmosphere. We use 35 ev of energy to form an ion pair and 1.2 NO_y formed per ion pair (see *Callis et al.*, [1991*a*] and references therein). As can be seen the energy fluctuations are sizeable.

Triangular symbols are the energy inputs to the atmosphere. In several instances, these energy inputs are shown to be higher (in terms of NO_y equivalents) than the total NO_y produced by the global oxidation of N_2O during a day. In most cases, the electron energy inputs are larger than the NO_y formation due to the N_2O above 50°latitude. Daily varying NO_y formation rate profiles are used as input in the 2-D simulations. We note that the formation rates above 80 km are underestimated since PET does not measure electrons with energies below 0.40 MeV. Consequently, we view these calculations as lower limits of the effect of electrons on stratospheric NO_y.

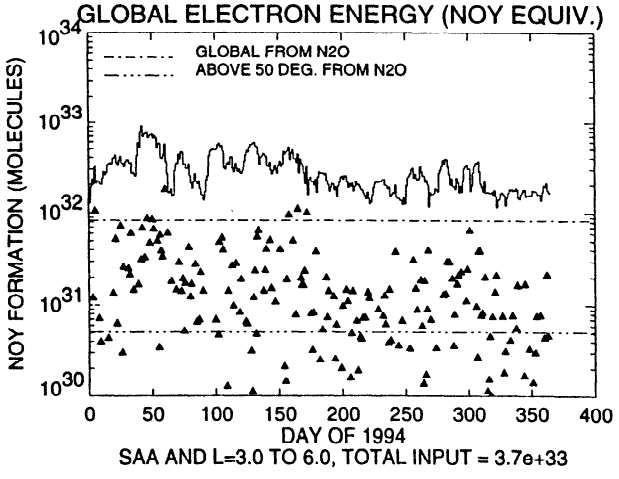

Figure 1. The solid line illustrates the variation of the GME for 1994. The triangles are atmospheric energy inputs. Dashed-dot lines indicate the NO_y molecules formed in a day by the oxidation of N_2O globally and above 50°in both hemispheres. Units are in NO_y molecules. See text for discussion.

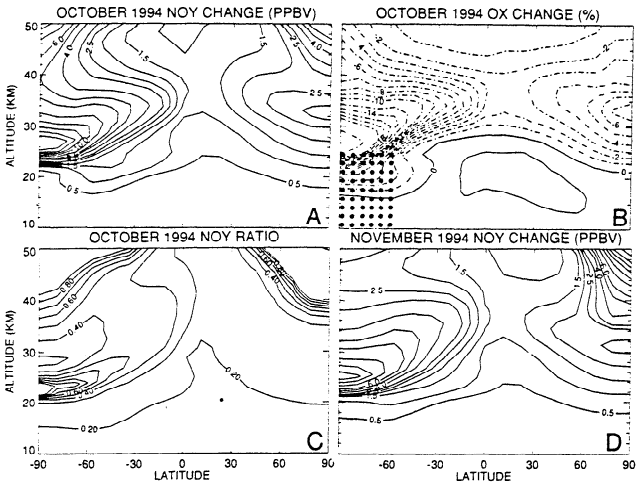

Figure 2. (*a*) The change in the mixing ratio of NO_y due to the effects of a thermospheric source and electrons (simulation 3) compared to the NO_y due to the oxidation of N_2O (simulation 1). (*b*) The percentage changes of O_3 due to the NO_y changes shown on (*a*). (*c*) Contours of R where, $R = (NO_{y,3} - NO_{y,2})/(NO_{y,2} - NO_{y,1})$ (See text). (*d*) Same as for (*a*) except for November 1994.

The HALOE, which is aboard the UARS (Upper Atmospheric Research Satellite) has been described by *Russell et al.* [1993]. Measurements of NO are made in occultation at sunrise and sunset. Normally, 15 profiles of each type are retrieved each day separated by ≈24°in longitude. Vertical coverage extends from 15 to 130 km for NO. Validation of the NO data has been reported by *Gordley et al.* [1995]. For simulations 2 and 3, we use an average of the sunrise and sunset NO observed by HALOE at 98.7 km for 911011 through 940926 as the upper boundary condition for NO_y. From 90°N to 90°S in 11.25°increments, the NO mixing ratios used are 2.2, 2.0, 1.6, 1.2, 0.6, 0.4, 0.3, 0.3, 0.3, 0.3, 0.3, 0.4, 0.6, 1.2, 1.6, 2.0, and 2.2. Units are 10^4 ppbv.

Results and Discussion

Simulation results for October 15 and November 15, 1994 are presented on Figures 2*a-d*. Panel 2*a* illustrates the October 15, 1994 NO_y mixing ratio difference between simulations 3 and 1. The largest increases occur at high latitudes. The significant increases at high northern latitudes, and at the high altitudes, indicate descent of NO_y which may occur during the northern fall, winter, and early spring.

Panel 2*b* illustrates the October 15, 1994 percentage changes in O_3 due to these NO_y increases. The simulations indicate O_3 depletions of 22% in mid August near 65°S and 33 km. By mid September, the depletions have reached ≈30% at 30 km and extend polewards of 75°S. Depletion reaches ≈30-35% by mid October at 27 km and is polewards of 75°-80°S. Values below 25 km are not reliable since a parameterization is used to prescribe the O_3 depletion due to heterogeneous chemistry on PSCs.

An examination of the three simulations permits an examination of the relative contributions of the thermospheric source and the electron NO source to the stratospheric NO_y increases. The ratio, $R = (NO_{y,3} - NO_{y,2})/(NO_{y,2} - NO_{y,1})$ is calculated from the three simulations and represents the ratio of NO_y increases between simulations 3 and 2 to the NO_y increases from simulations 2 and 1 and is shown on Figure 2*c*. Polewards of 60°S and above 20 km $0.3 \leq R \leq 1.0$ indicating that both sources of NO are important. Note, however, that the thermospheric NO observed by HALOE and used in the boundary condition also includes the effect of precipitating relativistic electrons [see *Callis et al.* 1996, this issue]. These effects cannot be separated out at this time. The parameter, R, will vary with time reflecting both relativistic electron variability, and thermospheric variations. Finally, panel 2*d* is similar to 2*a* except it is for November 15, 1994.

We turn now to the question of whether or not observational evidence exists to confirm the presence of the excess NO_y (NO_y beyond that due to N_2O oxidation) shown on Figures 2*a,d*. *Siskind and Russell* [1996] suggest that there is little evidence for significant transport of NO_y from the mesosphere to the stratosphere. Our own analysis of HALOE CH_4 and NO_x data is presented on Figures 3*a-c*. Figure 3*a* illustrates altitude-longitude contours of CH_4 mixing ratio near 73°S. Low values of CH_4, ≈0.2 to 0.3 ppmv above 25 km indicate air which has descended from the upper stratosphere or lower mesosphere.

Figure 3*b* shows a similar plot for the NO_x. Between 25 to 30 km and within the vortex, the NO_x of ≈11 ppbv are higher than would be expected to be associated with the relatively low CH_4. Figure 3*c*, for altitudes between 25 to 30 km, presents a scatter plot of NO_x and CH_4 observed by HALOE. Increasing NO_x with decreasing CH_4 at CH_4 less than 0.3 ppmv suggests a source of NO_x above 1 mbar other than N_2O oxidation. We suggest that *Siskind and Russell* [1996] did not find significant evidence of downward transport with the HALOE data because first, data wasn't available poleward of ≈50° during wintertime where the bulk of the NO_y is descending (also see Plate 1 of *Russell et al.* [1984]) and, second, by equinox, high latitude upper stratospheric NO_y originating in the mesosphere or above would have been photodissociated or dispersed.

Other independent evidence supports the presence of downward transport from the mesosphere. *Rinsland et al.* [1996] present ATMOS sunrise observations of total NO_y made during the ATLAS-3 mission for November

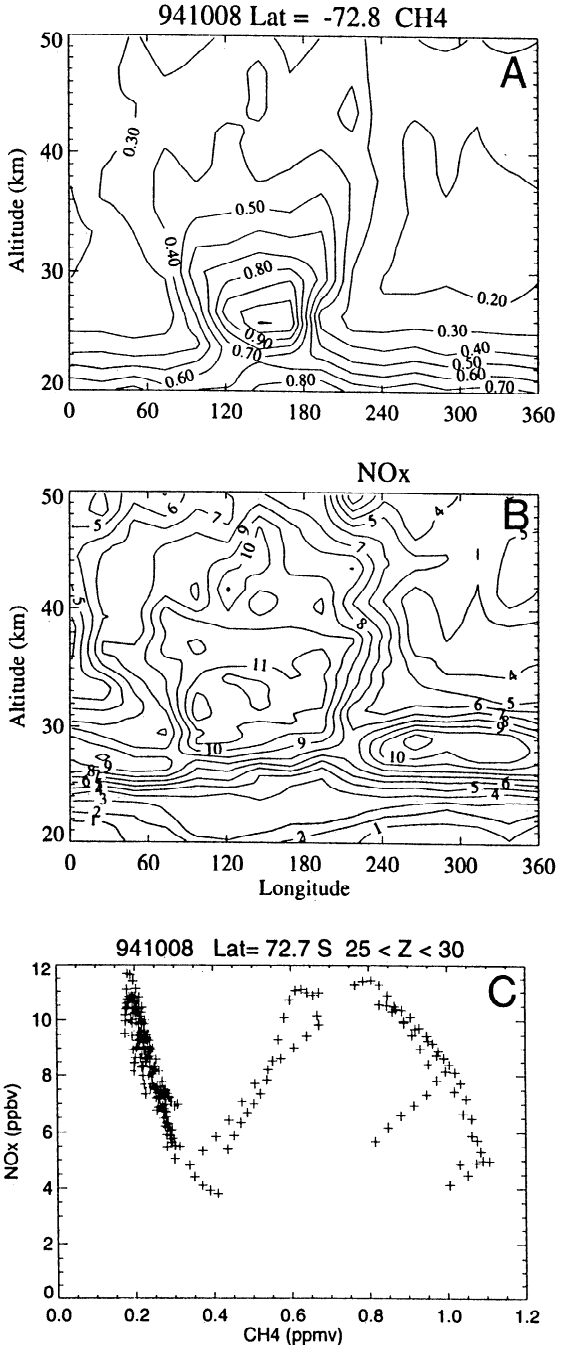

Figure 3. For sunset HALOE data: (*a*) Contour of CH_4 in ppmv for 941008. (*b*) Same as (*a*) except for NO_x (= NO + NO_2) in ppbv. (*c*) Scatter plot NO_x (ppbv) versus CH_4 (ppmv) for 941008 and for $25 \leq Z \leq 30$ km.

3-12, 1994 at 64.5°S to 72.4°S. They present ΔN, a measure of NO_y above or below that NO_y expected due to the oxidation of N_2O both inside and outside the polar vortex. Inside the vortex, and at altitudes of ≈25-30 km, values of ΔN (which we call excess NO_y) of up to 7 ppbv are found. These values are in excellent agreement, both in magnitude and location, with the results of the present simulation shown on Figure 2*d* and are consistent with the hypothesis that the positive

ΔN shown by *Rinsland et al.* within the vortex, and the high levels of NO_x at low CH_4 also within the vortex and shown on Figure 3, are due an NO_y source above the stratosphere followed by downward transport.

With regard to the October O_3 declines of $\approx$30-35% calculated and shown on Figure 2*b*, we hypothesize that the local O_3 reductions between 25-30 km reported by *Hofmann et al.* [1992] may be due to the same phenomenon (excess NO_y) occurring in 1991. *Hofmann et al.* conclude that these high altitude depletions extended over much, and possibly all of the vortex. Unfortunately, no low altitude electron measurements or thermospheric NO measurements are available for times which would permit a simulation for the 1991 period. Relative to the observations of Figure 3, we point out that O_3 observed by HALOE within the vortex between 25-30 km is $\approx$3 ppmv while that outside is $\approx$7 ppmv.

We conclude by noting that the current simulations, using NO observed by HALOE near 100 km as an upper boundary condition for NO_y, and using fluxes of relativistic electrons observed by SAMPEX suggest that downward transport of NO_y formed by thermospheric processes and by relativistic electron precipitation has significantly affected mid to lower stratospheric NO_y and O_3 mixing ratios during the austral spring in 1994. These results also: (1) appear to be consistent with an analysis of NO_x and CH_4 as observed by HALOE at 73°S in October 1994; (2) seem to offer an adequate explanation for the large positive levels of ΔN observed by ATMOS in November 1994 and reported by *Rinsland et al.* [1996]; and, (3) suggest an explanation for the large local O_3 depletions at 25-30 km observed in the antarctic spring and reported by *Hofmann et al.* [1992].

References

Baker, D. N., G. M. Mason, O. Figueroa, G. Colon, J. G. Watzin, and R. M. Aleman, An overview of the solar, anomalous, and magnetospheric particle explorer (SAMPEX) mission, IEEE Trans. on Geosci. and Remote Sensing, 31, 531, 1993.

Callis, L. B. and M. Natarajan, Ozone and nitrogen dioxide changes in the stratosphere during 1979-1984, Nature, 323, 772, 1986.

Callis, L. B., D. N. Baker, J. B. Blake, J. D. Lambeth, R. E. Boughner, M. Natarajan, R. W. Klebesadel, and D. J. Gorney, Precipitating relativistic electrons: Their long-term effect on stratospheric odd nitrogen levels, J. Geophys. Res., 96, 2939, 1991a.

Callis, L. B., R. E. Boughner, M. Natarajan, J. D. Lambeth, D. N. Baker, and J. B. Blake, Ozone depletion in the high latitude lower stratosphere: 1979–1990, J. Geophys. Res., 96, 2921, 1991b.

Callis, L. B., et al., Precipitating electrons: Evidence for effects on mesospheric odd nitrogen, Geophys. Res. Lett., In Press (this issue), 1996.

Cook, W. R. et al., PET: A proton/electron telescope for studies of magnetospheric, solar, and galactic particles, IEEE Trans. on Geosci. and Remote Sensing, 31, 565, 1993.

DeMore W. B. et al., Chemical kinetics and photochemical data for use in stratospheric modeling, Evaluation No. 10, *JPL Publication 92-20*, Jet Propulsion Laboratory, Pasadena, CA, 1992.

Garcia, R., S. Solomon, R. G. Roble, and D. W. Rusch, A numerical study of the response of the middle atmosphere to the 11-year solar cycle, Planet. Space Sci., 32, 411, 1984.

Gordley, L. L. et al., Validation of nitric oxide and nitrogen dioxide measurements made by HALOE for the UARS platform, J. Geophys. Res., 101, Accepted for Publication, 1995.

Hofmann, D. J., S. J. Oltmans, J. M. Harris, S. Solomon, T. Deshler, and B. J. Johnson, Observation and possible causes of new ozone depletion in Antarctica in 1991, Nature, 359, 283, 1992.

McIlwain, C. E., Coordinates for mapping the distribution of magnetically trapped particles, J. Geophys. Res., 66, 3681, 1961.

Mlynczak, M. G., and S. Solomon, A detailed evaluation of the heating efficiency in the middle atmosphere, J. Geophys. Res., 98, 10,517, 1993.

Rinsland, C. P., et al., ATMOS measurements of H_2O + $2CH_4$ and total reactive nitrogen in the November 1994 Antarctic stratosphere: Dehydration and denitrification in the vortex, Geophys. Res. Lett., 23, Accepted for Publication, 1996.

Russell, J. M., III, S. Solomon, L. L. Gordley, E. E. Remsberg, and L. B. Callis, The variability of stratospheric and mesospheric NO_2 in the polar winter night, J. Geophys. Res., 89, 7267, 1984.

Russell, J. M., A. F. Tuck, L. L. Gordley, J. H. Park, S. R. Drayson, J. E. Harries, R. J. Cicerone, and P. J. Crutzen, HALOE antarctic observations in the spring of 1991, Geophys. Res. Lett., 20, 719, 1993.

Siskind, David E. and James M. Russell, III, Coupling between middle and upper atmospheric NO: Constraints from HALOE observations, Geophys. Res. Lett., 23, 137, 1996.

Solomon, S., P. J. Crutzen, and R. G. Roble, Photochemical coupling between the thermosphere and lower atmosphere, 1, Odd nitrogen from 50 to 120 km, J. Geophys. Res., 87, 7206, 1982.

Yang, H., K. K. Tung, and E. Olaguer, Nongeostrophic theory of zonally averaged circulation. Part II: Eliassen-Palm flux divergence and isentropic mixing coefficient, J. Atmos. Sci., 47, 215, 1990.

Zhu, X., M. E. Summers, and D. F. Strobel, Calculation of CO2 15 micron band atmospheric cooling rates by curtis matrix interpolation of correlated-k coefficients, J. Geophys. Res., 97, 12,787, 1992.

(received November 7, 1995; revised May 1, 1996; accepted May 21, 1996.)